Identification of 3D shape from texture and motion across the visual field

Rick Gurnsey Department of Psychology, Concordia University, Montreal, QC, Canada

Frédéric J. A. M. Poirier Neurodynamics and Vision Lab-Centre for Vision Research, York University, Toronto, ON, Canada

Patricia Bluett Department of Psychology, Concordia University, Montreal, QC, Canada

Laurie Leibov Department of Psychology, Concordia University, Montreal, QC, Canada

Little is known about the perception of 3D shape in the visual periphery. Here we ask whether identification accuracy in shape-from-texture and shape-from-motion tasks can be equated across the visual field with sufficient stimulus magnification. Both tasks employed 3D surfaces comprising hills, valleys, and plains in three possible locations, yielding a 27 alternative forced-choice task (27AFC). Participants performed the task at eccentricities of 0 to 16 deg in the right visual field over a 64-fold range of stimulus sizes. Performance reached ceiling levels at all eccentricities, indicating that stimulus magnification was sufficient to compensate for eccentricity-dependent sensitivity loss. The parameter E_2 (in the equation $F = 1 + E / E_2$) was used to characterize the rate at which stimulus size must increase with eccentricity (E) to achieve foveal levels of performance. Three parameter models (μ, σ, and E_2) captured most of the variability in the psychometric functions relating stimulus size and eccentricity to accuracy for all participants' data in the two experiments. For the shape-from-texture task, the average E_2 was 1.52, and for the shape-from-motion task, it was 0.61. The E_2 values indicate that sensitivity to structure from motion declines at a faster rate with eccentricity than does sensitivity to structure from texture. Although size scaling with $F = 1 + E / E_2$ eliminated most eccentricity variation from the structure-from-motion data, there was some evidence that E_2 increases as accuracy decreases in the shape-from-texture task, suggesting that there may be more than one eccentricity-dependent limitation on performance in this task.

Keywords: motion, texture, 3D structure, eccentricity, cortical magnification, size scaling

Introduction

When visual stimuli of a constant size are moved into the visual periphery, our ability to resolve their details declines with increasing distance from the fovea (eccentricity). There are both theoretical and practical reasons for studying changes in visual sensitivity across the visual field. From a practical point of view, it is critical to understand the range of computations that can be performed in the visual periphery to inform rehabilitation programs that address the devastating effects of diseases such as macular degeneration. From a theoretical point of view, there has been a long-standing interest in quantifying changes in sensitivity across the visual field to understand the mechanisms that support various perceptual abilities. Over the years, there have been claims that the fovea is specialized for processing such properties as phase relationships (e.g., Rentschler & Treutwein, 1985) or integrating extended contours (Hess & Dakin, 1997), but such claims are frequently countered by evidence that performance in any task degrades gradually with eccentricity (Nugent, Keswani, Woods, & Peli, 2003) and can be offset by an appropriate stimulus magnification (Barrett, Morril, & Whitaker, 2000).

The magnification needed to offset an eccentricity-dependent sensitivity loss is often characterized by

$$S_E = S_0(1 + E/E_2), \quad (1)$$

where E_2 is the eccentricity (E) at which the stimulus size (S_E) must be doubled relative to a foveal standard (S_0) to achieve equivalent-to-foveal performance (Levi, Klein, & Aitsebaomo, 1985). E_2 can be derived from psychophysical experiments in which sensitivity is measured for a range of stimulus sizes and eccentricities (e.g., Sally & Gurnsey, 2001, 2003, 2004; Whitaker, Latham, Mäkelä, & Rovamo, 1993; Whitaker, Mäkelä, Rovamo, & Latham, 1992; Whitaker, Rovamo, MacVeigh, & Mäkelä, 1992). In such experiments, the function relating performance (e.g., thresholds or proportion correct responses) to size at each eccentricity can be collapsed onto a single psychometric function by dividing all actual stimulus sizes

doi: 10.1167/6.5.1 Received September 8, 2005; published April 12, 2006 ISSN 1534-7362

by $F = S_E / S_0 = 1 + E / E_2$ (Watson, 1987). E_2 is inversely related to the rate of sensitivity loss; large E_2 values represent gradual decreases in sensitivity with increases in eccentricity of stimulus presentation.

The rate of eccentricity-dependent sensitivity loss can be determined by both anatomical and physiological factors. Eccentricity-dependent stimulus magnifications using E_2 values of 3 deg or greater are generally thought to compensate for increases in cone spacing and decreases in ganglion cell density with eccentricity. Consequently, eccentricity-dependent sensitivity losses in tasks such as grating resolution (e.g., Rovamo & Virsu, 1979; Thibos, Still, & Bradley, 1996) can be compensated for by scaling the stimuli according to Equation 1 with E_2 values of 3 deg or greater.

Tasks producing smaller E_2 values (e.g., 2 deg and less) are not limited simply by the resolvability of the stimuli. Such tasks include orientation discrimination (Mäkelä, Whitaker, & Rovamo, 1993; Scobey, 1982), curvature detection (Whitaker et al., 1993), vernier acuity (Levi & Waugh, 1994; Whitaker, Rovamo, et al., 1992), phase discrimination (Morrone, Burr, & Spinelli, 1989), and symmetry detection (Barrett, Whitaker, McGraw, & Herbert, 1999; Sally & Gurnsey, 2001). Such tasks require the assessment of relative positions of the stimulus components and are therefore referred to as positional tasks. Positional tasks seem to be limited by cortical mechanisms because the assessment of relative position seems to require mechanisms having (at least) the computational structure of V1 simple cells. Furthermore, eccentricity-dependent changes in the cortical magnification factor (the amount of cortex, in millimeters, devoted to 1 deg of visual angle) are compensated for by size scaling with E_2 values of 1.5 or less. Although E_2 is difficult to estimate from physiological, electrophysiological, and imaging experiments, the weight of evidence suggests a value of 1.5 (Cowey & Rolls, 1974) or much less (e.g., Levi et al., 1985; Sereno et al., 1995; Slotnick, Klein, Carney, & Sutter, 2001; but see Dougherty et al., 2003, for much larger values, 3.67 deg on average).

It should be noted that a measured E_2 value cannot be unambiguously associated with a specific anatomical locus of resolution loss. For example, a given psychophysical task may be limited by several anatomical loci (Poirier & Gurnsey, 2002, 2005), and hence a single E_2 may not have a unique anatomical origin. Furthermore, the measured E_2 value can change with stimulus contrast within a single task. For example, Sally and Gurnsey (2003, 2004) found that E_2 increased as contrast decreased in an orientation discrimination task. A similar pattern can be inferred from the results of van de Grind, Koenderink, and van Doorn (1987) who showed that size-scaling stimuli with an E_2 of about 4 equated the functions relating motion thresholds (defined by SNR) to normalized velocity for eccentricities of 0 to 48 deg when RMS contrasts were greater than 10% to 20%. At lower contrasts, however, thresholds increased more at fixation than in the periphery. This suggests that if E_2 values were measured for specific normalized velocities, the results would be contrast dependent.

The vast majority of psychophysical studies of eccentricity-dependent sensitivity loss have employed stimuli that require detection or discrimination of two-dimensional stimuli, for example, grating detection, orientation discrimination, curvature detection, letter identification, vernier acuity, and symmetry detection. Furthermore, performance is most often measured at the limits of detection and discrimination (e.g., the smallest detectable orientation difference or the smallest detectable contrast). There has been almost no attention paid to questions of processing 3D shape across the visual field. For example, whether stimulus magnification (size scaling) is sufficient to equate 3D form perception across the visual field is unknown. In addition, it is not known to what extent scaling functions (i.e., Equation 1) might change with the level of accuracy that is to be matched between fovea and eccentric positions. From both practical and theoretical points of view, these represent serious gaps in our understanding of visual functioning across the visual field.

To our knowledge, there are two exceptions to the otherwise exclusive focus on perception of 2D form. First, Melmoth, Kukkonen, Mäkelä, and Rovamo (2000) had participants perform a face identification task for a range of sizes and eccentricities. For each stimulus size and eccentricity, they varied stimulus contrast to determine face identification thresholds. Melmoth et al. found that contrast thresholds came to different asymptotic levels at each eccentricity. Therefore, the conditions necessary to perform a classic size-scaling analysis (e.g., Mäkelä et al., 1993) were not met. In fact, Melmoth et al. found that stimuli had to be scaled for both size and contrast for psychometric functions to be equated across the visual field. It is not clear from this study what was required of participants' internal representations of the stimuli to perform the task at threshold levels of contrast. For example, with practice, small 2D fragments of the stimuli might serve to distinguish faces sufficiently to achieve threshold-level performance.

In a second example, Ikeda, Blake, and Watanabe (2005) studied the identification of biological motion (i.e., point walker displays, Johansson, 1973) across the visual field. They varied stimulus size and eccentricity and measured the number of noise dots in the stimulus required to elicit threshold-level performance. Their principal finding was that for no stimulus size did sensitivity at 4 and 12 deg eccentricity reach the same level found at the fovea. This result resembles that of Melmoth et al. (2000) in that neither contrast thresholds nor noise thresholds reach the same asymptotic levels across the visual field.

The present experiments were conducted to address the basic question: Can the identification of 3D shapes be equated across the visual field by an appropriate magnification of the stimulus? How should this question be addressed?

There have been a number of interesting methods developed to assess accuracy of depth perception (for a review, see Todd, 2004). Many of these tasks require participants to estimate local 3D structure at many points on the same object. A surface can then be constructed that is

maximally consistent with these local estimates. Estimates of local 3D structure can be made by (a) having participants make judgments about depth minima and maxima along a scan line across an object's surface (e.g., Todd, Oomes, Koenderink, & Kappers, 2004), (b) having participants adjust the apparent slant and tilt of circle until it appears to lie in the tangent plane of an object's surface at a designated point (e.g., Koenderink, van Doorn, & Kappers, 1992, Koenderink, van Doorn, Kappers, & Todd, 2001; Todd, Koenderink, van Doorn, & Kappers, 1996), or (c) having participants convey through analog response the perceived depth at each of n equally spaced points along an object's surface (e.g., Koenderink et al., 2001; Todd et al., 2004). These tasks reveal that observers can make use of depth cues such as shading and texture deformations to derive consistent and qualitatively correct interpretations of 3D surface shape, although the absolute magnitude of depth modulations may be underestimated (Todd et al., 2004).

Unfortunately, such tasks are difficult to adapt to our present needs because they require relatively long exposures to the stimulus and a large number of measurements are necessary for each stimulus. Furthermore, they actually produce too much information in response to our relatively simple question about the identification of 3D shape across the visual field. To our knowledge, no previous studies have addressed the question of whether 3D surface shape can be identified with high accuracy across the visual field; that is, it may be that gross differences in 3D shape cannot be distinguished in the periphery. Therefore, to ask our first-order question, we require a simpler task that requires the extraction of depth that can be accomplished with brief exposures and that produces tractable results.

The task and stimuli we employed were adapted from those used by Sperling, Dosher, and Landy (1990). Each stimulus comprised three regions arranged as the vertexes of an equilateral triangle, and each region could be a hill, valley, or plain. Figure 1 depicts one such stimulus. Three regions, each with three possible values, give rise to 27 different stimuli. In one experiment, the 3D surfaces were conveyed by texture (Figure 1), and in another, they were conveyed by relative motion (i.e., the kinetic depth effect, Wallach & O'Connell, 1953). Therefore, the participants' task was to identify which of the 27 stimuli had been presented on a given trial (27 alternative forced-choice task; 27AFC). Stimuli were presented at a range of sizes and eccentricities. This method has been used in several previous studies (e.g., Barrett, Morrill, & Whitaker, 2000; Saarinen, 1988; Sally & Gurnsey, 2001, 2003).

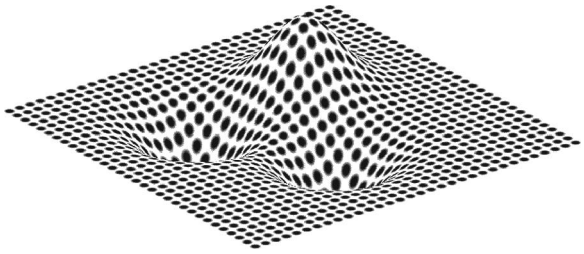

Figure 1. An example of a shape-from-texture stimulus.

We had three related questions: (1) Can 3D shape identification be equated across the visual field by appropriate size scaling? We would expect that as stimulus size increases, shape identification should improve at each eccentricity. If size scaling can eliminate all or most eccentricity-dependent variation from the data, the size versus performance curves should be identical except for position when plotted on a logarithmic axis. (2) If size scaling can eliminate all eccentricity-dependent variance from the data, what are the E_2 values that characterize each task and are these the same? (3) What might the recovered E_2 values tell us about the mechanisms that support the perception of 3D shape?

Method

Participants

The participants included three of the authors (R.G., P.B., and L.L.) and six volunteers recruited from the vision laboratory at Concordia. Ages ranged from 21 to 51, and six of the nine participants were women. All participants reported normal or corrected-to-normal vision and wore the appropriate distance correction during testing.

Apparatus

Stimulus presentation and data collection were under the control of a Macintosh G4 computer equipped with a 21-in. multiscan monitor. A chin rest was used to steady participants' gaze.

Stimuli

Stimuli were created using MATLAB (Mathworks, Ltd.) and the Psychophysics Toolbox extensions (Brainard, 1997; Pelli, 1997).

Shape from texture

Each stimulus was created by texture mapping a 32×32 array of dots (each of which was defined within a 16×16 pixel window and had a diameter of 11 pixels) onto a 512×512 surface having 1 of the 27 possible topographies. The resulting surface was orthographically projected to the image plane. The horizontal extent of each stimulus was 512 pixels. The actual stimulus size was determined by viewing distance and screen resolution. An example of this stimulus is shown in Figure 1.

Shape from motion

The 27 surfaces were created within a 256 × 256 array; 1,024 points on the surface were randomly chosen to project to the image. A small, black Gaussian blob (SD = 1.25 pixels) was centered on each of these 1,024 points. The surface was tilted 45 deg to the line of sight, and each dot was orthographically projected to the image plane with hidden surface removal. The stimulus rotated through 60 deg (−30 to 30) about the Z-axis (height) in 30 equal steps. For a viewing angle of 0 deg, the horizontal extent of the stimulus was 256 pixels. The actual stimulus size was determined by viewing distance and screen resolution. Figure 2 provides an example of the shape-from-motion stimulus.

Stimulus size and eccentricity

For both tasks, stimulus size was varied by a combination of viewing distance and screen resolution. At viewing distances of 28.5, 57, 114, 228, or 456 cm, the screen resolution was set to the highest possible value (1,600 horizontal pixels, with pixel size approximately 0.24 mm). At 28.5 cm, testing was also conducted with the screen resolution halved (800 horizontal pixels, with pixel size approximately 0.48 mm). At 456 cm, testing was also conducted with stimuli subsampled by a factor of 2, thus mimicking a viewing distance of 912 cm. The combined effects of viewing distance and screen resolution provided a 64-fold range of stimulus sizes. The differences in stimulus structure between the two experiments make specifying a common metric for stimulus size in terms of the carriers (texture and motion) of the 3D shape somewhat difficult. However, we can express size in terms of the separation between topographical features when surface slant is perpendicular to the line of sight. In the case of motion, the seven sizes were 0.13, 0.26, 0.52, 1.03, 2.06, 4.12, and 8.20 deg of visual angle. In the case of texture, sizes (as just defined) were twice those for motion. For simplicity, in what follows, we describe performance in terms of relative stimulus size.

Figure 2. An example of a shape-from-motion stimulus. (This image depicts the first frame of the surface shown in Figure 1. Click on the image to view the movie.)

The stimuli were always presented at the center of the computer monitor, and the fixation spot was varied to control eccentricity of stimulus presentation. Stimuli were presented at 0, 1, 2, 4, 8, and 16 deg in the right visual field on the horizontal meridian. The fixation point was a small green dot on the computer screen when possible, and a small luminous red dot positioned at the appropriate distance off the screen otherwise. Eccentricity was defined relative to the center of the stimulus. (Note that we did not attempt to modify the stimuli to compensate for perspective distortions that might arise from changes in viewing distance or eccentricity. Because such distortions would not change the qualitative interpretation of a surface, e.g., two hills and a valley, this seems a reasonable simplification to address our fundamental question.)

In the shape-from-motion conditions, the presentation of the 30 frames also took 352 ms on a monitor with a frame rate of 85 Hz. Each stimulus in the shape-from-texture condition was also presented for 352 ms. All stimuli were presented at the maximum available contrast. The color-lookup table of the monitor was linearized using routines available in the Psychophysics Toolbox.

Procedure

Participants were seated in front of the computer screen with their heads in a chin rest and asked to fix their gaze on the fixation point during stimulus presentation. Immediately following the presentation of the stimulus, the participant entered a code to identify the stimulus. A valley was coded as a 1, a plain as a 2, and a hill as a 3. The arrangement of the three locations formed an inverted triangle, and participants reported the top two locations (left to right) followed by the bottom location. The appropriate response for the stimulus shown in Figure 1 would be [1, 3, 1]. Participants had an opportunity to correct their responses before entering them into the computer. Feedback about the correctness of a response was given in the form of a 200-ms, 300-Hz beep following each error. Participants were told to be as accurate as possible and that response time is not measured. Before beginning the experiment, each participant was permitted to practice until the response coding was perfectly learned.

For each stimulus size, eccentricities were tested from smallest (0 deg) to largest (16 deg) in order. Viewing distances were tested in random order. At each eccentricity, each of the 27 stimuli was presented three times in a random order for a total of 81 trials per eccentricity per size.

Results

For each participant, the proportion of correct responses was computed for each eccentricity and stimulus size. The raw data for the shape-from-texture experiment are

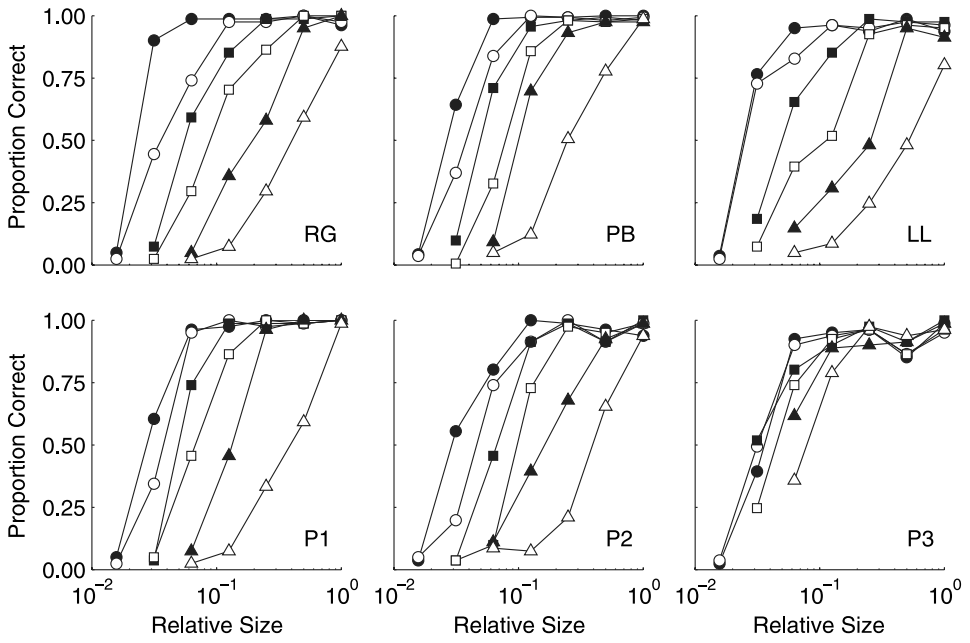

Figure 3. Raw data from the shape-from-texture experiment; 0 deg (filled circles), 1 deg (unfilled circles), 2 deg (filled squares), 4 deg (unfilled squares), 8 deg (filled triangles), 16 deg (unfilled triangles).

summarized in Figure 3. Performance improved as stimulus size increased in all cases. The curves have generally the same shape at each eccentricity and shift to the right as eccentricity increases. The data from Participant 3 (P3) substantially differ from those of the remaining participants and suggest that he was not maintaining fixation as eccentricity increased. In almost all cases, performance reached 100% correct responses even at the greatest eccentricities. Therefore, depth can be recovered from texture in the periphery if stimuli are sufficiently magnified. To quantify the rate at which stimuli must be scaled with eccentricity, we calculated the E_2 value required to collapse data from all eccentricities onto a single psychometric function. The accuracy data at each eccentricity were assumed to be well described by a Gaussian integral normalized to the range of 1/27 (chance) to 1 when plotted against the logarithm of stimulus size. A mean (μ_E) and standard deviation (σ_E) characterize the function at each eccentricity (E). Assuming that all σ_E

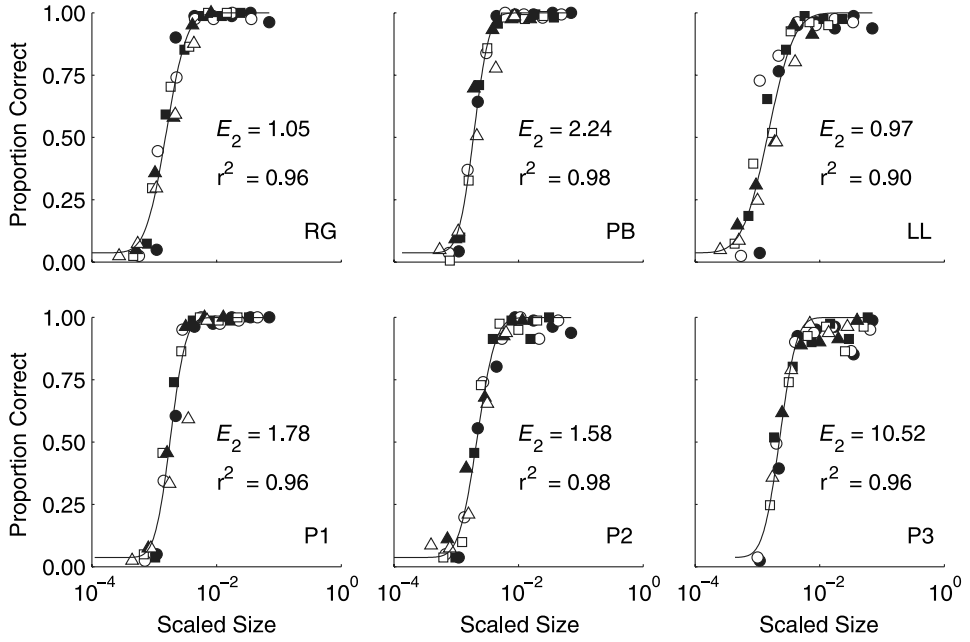

Figure 4. Data from the shape-from-texture experiment collapsed onto the best fitting function for each participant. The E_2 value and proportion of explained variance are shown for each participant.

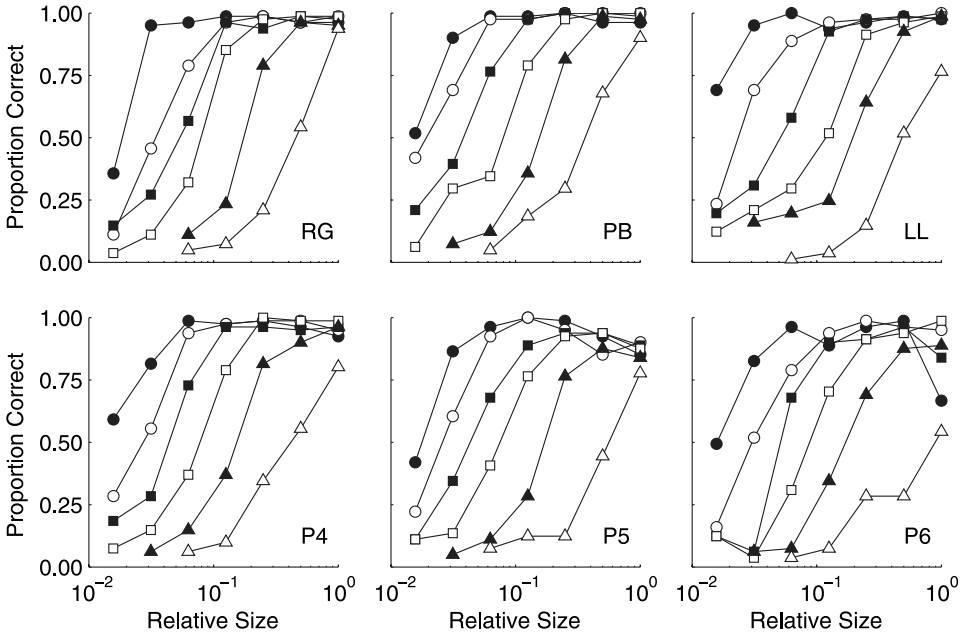

Figure 5. Raw data from the shape-from-motion experiment; 0 deg (filled circles), 1 deg (unfilled circles), 2 deg (filled squares), 4 deg (unfilled squares), 8 deg (filled triangles), 16 deg (unfilled triangles).

are the same, the changes in μ_E with eccentricity should correspond to a shift along the log-size axis such that $\mu_E = \log(F_E) + \mu_0$, where $F_E = 1 + E / E_2$. Therefore, if the appropriate E_2 is available, all data should collapse to a single function by subtracting $\log(F_E)$ from the logarithm of stimulus size at each eccentricity. In other words, three parameters (μ_0, σ_E, and E_2) should be sufficient to explain most of the variability in the data. We used an error minimization procedure (fminsearch) available in MATLAB to find the best fitting values of μ_0, σ_E, and E_2 for each participant. The results are summarized in Figure 4.

On average, the fits explained 96% of the variability in the raw data. Excluding P3, the average E_2 value was 1.52 with an estimated standard error of 0.53. Therefore, the 95% confidence interval for E_2 ranges from 0.79 to 2.25.

The results of the shape-from-motion experiment are summarized in Figure 5, and the fits are shown in Figure 6.

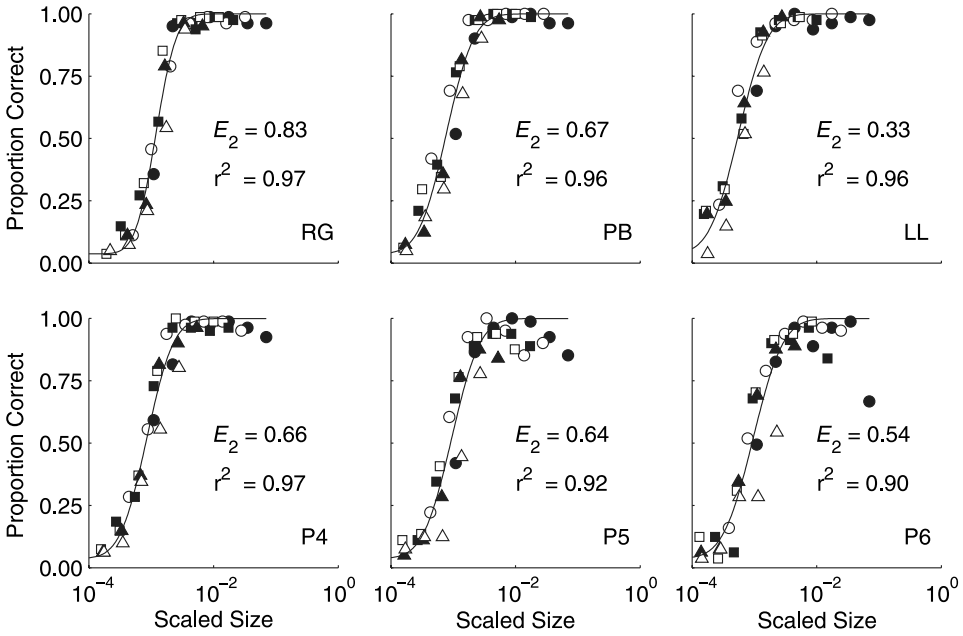

Figure 6. Data from the shape-from-motion experiment collapsed onto the best fitting function for each participant. The E_2 value and proportion of explained variance are shown for each participant.

As before, performance improved as stimulus size increased. The curves have generally the same shape at each eccentricity and are shifted to the right as eccentricity increases. As with the shape-from-texture experiment, we sought to quantify the size scaling required to collapse data from all eccentricities onto a single curve for each participant. On average, the fits explained 95% of the variability in the raw data. The average E_2 value was 0.61 with an estimated standard error of 0.17. Therefore, the 95% confidence interval for E_2 ranges from 0.42 to 0.81.

The E_2 values from the two experiments were submitted to a two-sample t test, and the difference between the two means proved to be statistically significant, $t(9) = 4.04$, $p < .005$.

To assess whether our data-fitting method significantly biased our results, we fit the data for each participant and each eccentricity with a cumulative Gaussian. Threshold values obtained in this way linearly increased with eccentricity; on average, linearity explained 97% of the variability in the thresholds. Using these thresholds to compute E_2, we found average values of 1.41 for the texture experiment and 0.55 for the motion experiment. These thresholds were not significantly different from those reported earlier, $t(4) = 1.95$ and $t(5) = 1.26$ for texture and motion, respectively, which corresponded to effect sizes (Hedges g) of 0.87 and 0.51.

The *slopes* of the best fitting functions were submitted to a within-participants analysis of variance. There was a significant increase in slopes with eccentricity, $F(4, 20) = 3.79$, $p < .05$, for the texture experiment (eccentricity explained 43% of the variability in the slopes) but not for the motion experiment, $F(5, 25) = 1.46$, $p > .05$ (eccentricity explained 18% of the variability in the slopes). Therefore, in the texture experiment, the assumption that the psychometric functions differ only in terms of position on the log-size axis is shown to be incorrect. The implication of this violation is that the E_2 value is dependent on the performance level that is being matched across eccentricities. E_2 values recovered from low performance levels (smaller stimuli) will be larger than E_2 values recovered from high performance levels.

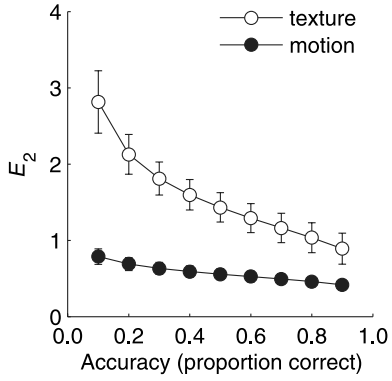

Figure 7. Plot of E_2 as a function of accuracy for the texture ($n = 5$) and motion ($n = 6$). Error bars represent ±*SEM*.

To illustrate this point, we used the best fitting psychometric functions to determine the stimulus size that elicited a fixed accuracy at each eccentricity for both motion and texture experiments. From these sizes, we were able to compute E_2 values for each of nine levels of accuracy (proportion correct ranging from 0.1 to 0.9 in equal linear steps). The results are plotted in Figure 7 (the texture results exclude P3). In both cases, average E_2 values decrease as performance level increases; however, the decrease is far more substantial in the texture experiment. In the case of texture, the average E_2 values calculated at different levels of accuracy ranged from 2.82 to 0.89, and in the case of motion, the average E_2 values ranged from 0.78 to 0.41. There is far greater variability in the case of texture than motion. Therefore, the average E_2 values derived from the three-parameter model in the case of motion (average $E_2 = 0.61$) are more representative of the accuracy-dependent E_2 values than in the case of texture (average $E_2 = 1.52$).

General discussion

We asked if size scaling would be sufficient to equate identification of shape from texture and motion across the visual field, and we found out that it is. It is interesting to note that there was no evidence that performance reached different asymptotic levels at greater eccentricities, as was found by Melmoth et al. (2000) in a face identification task. Therefore, within the limits of the sizes and eccentricities tested here, performance reaches ceiling at almost all eccentricities if stimuli are sufficiently magnified.

The average E_2 values (derived from the three parameter model) differed significantly and revealed greater losses with increased eccentricity for shape from motion (mean $E_2 = 0.61$) than for shape from texture (mean $E_2 = 1.52$). However, for the texture data, the model fit can be improved by allowing for the slope of the best fitting functions to change with eccentricity. The results show that the recovered E_2 value depends on the level of accuracy that is to be equated across eccentricities. This change in E_2 with accuracy level is far less pronounced in the case of motion.

To understand the different E_2 values recovered for texture and motion, it may be useful to distinguish between the medium that *carries* the 3D shape (luminance variations in the case of shape from texture and relative motions in the case of shape from motion) and the mechanism that integrates information from the carrier to produce a representation of 3D shape (i.e., extracting 3D shape from the density and shapes of the dots in the case of structure from texture and the speed gradients in the case of structure from motion). It is possible for E_2 values to reflect eccentricity-dependent limitations associated with the carrier or the integrative function; these may not be identical within a particular task. Therefore, different E_2 values associated with texture and motion might reflect factors associated with the carrier, the integrative functions, or both. In

addition, it might be that the integrative functions are specific to a particular medium so that they do not necessarily produce the same E_2 value.

Texture in the present stimuli was a combination of dot density and deformations due to surface slant. Both of these would be limited by sampling density of the retina, and therefore resolution may limit performance as stimulus size decreases. Thus, as performance drops (i.e., as stimuli become smaller), there may be two contributions to performance, namely, the quality of the input to the shape-from-texture calculation and the integrative ability of the shape-from-texture calculation itself. As stimulus size increases, one would expect that only the integrative ability of the shape-from-texture calculation limits performance. One could speculate that the change from integrative limitations to resolution limitations with decreasing stimulus size (and accuracy) corresponds to a change from cortical to retinal limitations. (This is the same argument made by Sally & Gurnsey, 2003, with respect to *performance-level*-dependent changes; e.g., Figure 7, in the E_2 value associated with orientation discrimination. Poirier & Gurnsey, 2002, 2005, have also argued that multiple factors may limit performance and that the relative influences of different factors might change with stimulus size and eccentricity.)

Shape in the motion experiment was conveyed by relative motion, and scaling functions associated with motion are relatively flat (i.e., large E_2 values; Whitaker, Mäkelä, et al., 1992). This means that the carrier for shape in the motion experiment should not be greatly affected by eccentricity even at the smaller stimulus sizes. Therefore, it is reasonable to think that in the structure-from-motion experiment, the main limitation at all stimulus sizes should be at the integrative level rather than at the resolution level. Therefore, one could speculate that at all levels of accuracy, the principal limitation in structure from motion corresponds to cortical mechanisms.

As mentioned, it seems reasonable to assume that at the largest stimulus sizes, the principal limitation on performance is the ability of the visual system to integrate information from the carrier to recover a representation of 3D structure. It is interesting to note that in Figure 7, the two curves do not appear to converge to the same asymptotic E_2 value. Even at 90% correct responses, the E_2 values are lower for motion than for texture. In other words, in the (presumed) absence of limitations on resolving the carrier, the scaling gradient is steeper in the case of motion than texture. Therefore, there appear to be differences in eccentricity-dependent limitations on the mechanisms that recover structure from motion and structure from texture.

Of course, these differences may arise from differences in mechanisms in the ventral and dorsal streams. Specifically, the motion task may be limited by mechanisms in the dorsal stream, whereas the texture task may be limited by mechanisms in the ventral stream. On this assumption, it seems that sensitivity to 3D structure falls off more quickly with eccentricity in the ventral stream than in the dorsal stream.

Our data may be seen as inconsistent with those of Ikeda et al. (2005), who concluded that perception of biological motion is unscalably poor in the periphery. One might argue that the differences in our results and theirs reflect task differences; biological-motion computations may be subject to different limitations than structure-from-motion computations. Alternatively, it might be that methodological differences (particularly those relating to how performance was limited; noise in the case of Ikeda et al., 2005, and size alone in this study) explain the apparent discrepancy. If we were to repeat this study and measure noise tolerance at each stimulus size and eccentricity, we might find, as did Ikeda et al., that peak sensitivity at fixation is never matched in the periphery, or if we replicated their experiment but measured accuracy as a function of size (and eccentricity), we might replicate the present findings.

It is certainly straightforward to determine if differences in task or methodology account for the different results under conditions that might be expected to involve similar computational requirements. In fact, a recent report by Gibson, Sadr, Troje, and Nakayama (2005) provides evidence consistent with the critical role of noise in size scaling. Gibson et al. had participants decide whether point-light walkers were moving to the right or left at eccentricities of 0, 10, 20, and 40 deg in the right visual field. Stimuli were presented at six sizes at each eccentricity. It was found that size scaling with E_2 values of about 3.5 on average was sufficient to equate performance across the visual field.

The fact that size scaling alone is insufficient to equate noise resistance between fovea and periphery in the Ikeda et al. (2005) study does not mean that the task is unscalably poor in the periphery. As noted by Yager and Davis,

> [the] parameter values of many visual functions are different, depending on the distance and direction from the fovea at which they are estimated. These changes cannot be attributed to a uniform change in the local scale for all functions because different functions … do not co-vary across the visual field with anything approaching perfect correlation (Yager & Davis, 1987).

Thus, the local scale of mechanisms may change with eccentricity at one rate, and the noise sensitivity of the mechanisms may change at another rate. The eventual goal should be to characterize these two limitations on performance as a function of eccentricity (Melmoth et al., 2000; Melmoth & Rovamo, 2003; Poirier & Gurnsey, 2002, 2005; Strasburger, Harvey, & Rentschler, 1991; Strasburger, & Rentschler, 1996; Strasburger, Rentschler, & Harvey, 1994). The present results hint at two limitations on performance in the case of shape from texture but not in the case of shape from motion. The changing effects of noise across eccentricity for the present tasks deserve further study. It is quite likely that an increase in noise sensitivity across the visual field is related to the increase in crowding effects with eccentricity (e.g., Latham & Whitaker, 1996).

The present experiment has shown that 3D shapes can be accurately identified across the visual field. However, this does not necessarily mean that the perception of 3D shape was identical for all conditions eliciting the same level of performance. As mentioned, we did not attempt to compensate for quantitative distortions of the 3D shape that might arise from changes in viewing distance and eccentricity. Given that the present results suggest that size scaling can compensate for eccentricity-dependent sensitivity losses, subsequent research can address the question of whether there are quantitative changes in perceived shape with eccentricity.

Conclusions

Stimulus magnification is sufficient to equate the identification of structure from motion and structure from texture across the visual field. There is little evidence that double scaling is needed in the case of structure from motion and, on average, that an E_2 value of 0.61 is sufficient to equate performance across the visual field. The situation is slightly more complicated in the case of structure from texture. Because the slopes of the psychometric functions increased with eccentricity, the E_2 value of 1.52 appears to represent the combined effects of limitations at different stimulus sizes. When stimuli are large and low-level resolution does not limit performance, E_2 values are larger in a structure-from-texture task than in a structure-from-motion task. These different E_2 values may represent different eccentricity-dependent changes in sensitivity to 3D shape in the ventral and dorsal pathways.

Acknowledgments

This research was supported by an NSERC grant to Rick Gurnsey. We are grateful for the helpful comments of two anonymous reviewers.

Commercial relationships: none.
Corresponding author: Rick Gurnsey.
Email: Rick.Gurnsey@concordia.ca.
Address: Department of Psychology, Concordia University, 7141 Sherbrooke St. West, Montreal, Quebec, Canada H4B 1R6.

References

Barrett, B. T., Morrill, P., & Whitaker, D. (2000). Compound grating discrimination in extrafoveal and amblyopic vision. *Experimental Brain Research, 131,* 225–235. [PubMed]

Barrett, B. T., Whitaker, D., McGraw, P. V., & Herbert, A. M. (1999). Discriminating mirror symmetry in foveal and extra-foveal vision. *Vision Research, 39,* 3737–3744. [PubMed]

Brainard, D. H. (1997). The Psychophysics Toolbox. *Spatial Vision, 10,* 433–436. [PubMed]

Cowey, A., & Rolls, E. T. (1974). Human cortical magnification factor and its relation to visual acuity. *Experimental Brain Research, 21,* 447–454. [PubMed]

Dougherty, R. F., Koch, V. M., Brewer, A. A., Fischer, B., Modersitzki, J., & Wandell, B. A. (2003). Visual field representations and locations of visual areas V1/2/3 in human visual cortex. *Journal of Vision, 3*(10), 586–598, http://journalofvision.org/3/10/1/, doi:10.1167/3.10.1. [PubMed] [Article]

Gibson, L. A., Sadr, J., Troje, N. F., & Nakayama, K. (2005). Perception of biological motion at varying eccentricity [Abstract]. *Journal of Vision, 5*(8), 16a, http://journalofvision.org/5/8/16/, doi:10.1167/5.8.16.

Hess, R. F., & Dakin, S. C. (1997). Absence of contour linking in peripheral vision. *Nature, 390,* 602–604. [PubMed]

Ikeda, H., Blake, R., & Watanabe, K. (2005). Eccentric perception of biological motion is unscalably poor. *Vision Research, 45,* 1935–1943. [PubMed]

Johansson, G. (1973). Visual perception of biological motion and a model for its analysis. *Perception and Psychophysics, 14,* 201–211.

Koenderink, J. J., van Doorn, A. J., & Kappers, A. M. (1992). Surface perception in pictures. *Perception & Psychophysics, 52,* 487–496. [PubMed]

Koenderink, J. J., van Doorn, A. J., Kappers, A. M., & Todd, J. T. (2001). Ambiguity and the 'mental eye' in pictorial relief. *Perception, 30,* 431–448. [PubMed]

Latham, K., & Whitaker, D. (1996). Relative roles of resolution and spatial interference in foveal and peripheral vision. *Ophthalmic and Physiological Optics, 16,* 49–57. [PubMed]

Levi, D. M., Klein, S. A., & Aitsebaomo, A. P. (1985). Vernier acuity, crowding and cortical magnification. *Vision Research, 25,* 963–977. [PubMed]

Levi, D. M., & Waugh, S. J. (1994). Spatial scale shifts in peripheral vernier acuity. *Vision Research, 34,* 2215–2238. [PubMed]

Mäkelä, P., Whitaker, D., & Rovamo, J. (1993). Modelling of orientation discrimination across the visual field. *Vision Research, 33,* 723–730. [PubMed]

Melmoth, D. R., Kukkonen, H. T., Mäkelä, P. K., & Rovamo, J. M. (2000). The effect of contrast and size scaling on face perception in foveal and extrafoveal vision. *Investigative Ophthalmology & Visual Science, 41,* 2811–2819. [PubMed] [Article]

Melmoth, D. R., & Rovamo, J. M. (2003). Scaling of letter size and contrast equalizes perception across eccentricities and set sizes. *Vision Research, 43,* 769–777. [PubMed]

Morrone, M. C., Burr, D. C., & Spinelli, D. (1989). Discrimination of spatial phase in central and peripheral vision. *Vision Research, 29,* 433–445. [PubMed]

Nugent, A. K., Keswani, R. N., Woods, R. L., & Peli, E. (2003). Contour integration in peripheral vision reduces gradually with eccentricity. *Vision Research, 43,* 2427–2437. [PubMed]

Pelli, D. G. (1997). The VideoToolbox software for visual psychophysics: Transforming numbers into movies. *Spatial Vision, 10,* 437–442. [PubMed]

Poirier, F. J., & Gurnsey, R. (2002). Two eccentricity-dependent limitations on subjective contour discrimination. *Vision Research, 42,* 227–238. [PubMed]

Poirier, F. J., & Gurnsey, R. (2005). Non-monotonic changes in performance with eccentricity modeled by multiple eccentricity-dependent limitations. *Vision Research, 45,* 2436–2448. [PubMed]

Rentschler, I., & Treutwein, B. (1985). Loss of spatial phase relationships in extrafoveal vision. *Nature, 313,* 308–310. [PubMed]

Rovamo, J., & Virsu, V. (1979). An estimation and application of the human cortical magnification factor. *Experimental Brain Research, 37,* 495–510. [PubMed]

Saarinen, J. (1988). Detection of mirror symmetry in random dot patterns at different eccentricities. *Vision Research, 28,* 755–759. [PubMed]

Sally, S., & Gurnsey, R. (2001). Symmetry detection across the visual field. *Spatial Vision, 14,* 217–234. [PubMed]

Sally, S. L., & Gurnsey, R. (2003). Orientation discrimination in foveal and extra-foveal vision: Effects of stimulus bandwidth and contrast. *Vision Research, 43,* 1375–1385. [PubMed]

Sally, S. L., & Gurnsey, R. (2004). Orientation discrimination across the visual field: Matching perceived contrast near threshold. *Vision Research, 44,* 2719–2727. [PubMed]

Scobey, R. P. (1982). Human visual orientation discrimination. *Journal of Neurophysiology, 48,* 18–26. [PubMed]

Sereno, M. I., Dale, A. M., Reppas, J. B., Kwong, K. K., Belliveau, J. W., Brady, T. J., et al. (1995). Borders of multiple visual areas in humans revealed by functional magnetic resonance imaging. *Science, 268,* 889–893. [PubMed]

Slotnick, S. D., Klein, S. A., Carney, T. & Sutter, E. E. (2001). Electrophysiological estimate of human cortical magnification. *Clinical Neurophysiology, 112,* 1349–1356. [PubMed]

Sperling, G., Dosher, B. A., & Landy, M. S. (1990). How to study the kinetic depth effect experimentally. *Journal of Experimental Psychology: Human Perception and Performance, 16,* 445–450. [PubMed]

Strasburger, H., Harvey, L. O., Jr., & Rentschler, I. (1991). Contrast thresholds for identification of numeric characters in direct and eccentric view. *Perception & Psychophysics, 49,* 495–508. [PubMed]

Strasburger, H., & Rentschler, I. (1996). Contrast-dependent dissociation of visual recognition and detection fields. *European Journal of Neuroscience, 8,* 1787–1791. [PubMed]

Strasburger, H., Rentschler, I., & Harvey, L. O., Jr. (1994). Cortical magnification theory fails to predict visual recognition. *European Journal of Neuroscience, 6,* 1583–1587. [PubMed]

Thibos, L. N., Still, D. L., & Bradley, A. (1996). Characterization of spatial aliasing and contrast sensitivity in peripheral vision. *Vision Research, 36,* 249–258. [PubMed]

Todd, J. T. (2004). The visual perception of 3D shape. *Trends in Cognitive Sciences, 8,* 115–121. [PubMed]

Todd, J. T., Koenderink, J. J., van Doorn, A. J., & Kappers, A. M. (1996). Effects of changing viewing conditions on the perceived structure of smoothly curved surfaces. *Journal of Experimental Psychology: Human Perception and Performance, 22,* 695–706. [PubMed]

Todd, J. T., Oomes, A. H., Koenderink, J. J., & Kappers, A. M. (2004). The perception of doubly curved surfaces from anisotropic textures. *Psychological Science, 15,* 40–46. [PubMed]

van de Grind W. A., Koenderink, J. J., & van Doorn, A. J. (1987). Influence of contrast on foveal and peripheral detection of coherent motion in moving random-dot patterns. *Journal of the Optical Society of America A, Optics and Image Science, 4,* 1643–1652. [PubMed]

Wallach, H., & O'Connell, D. N. (1953) The kinetic depth effect. *Journal of Experimental Psychology, 45,* 205–217. [PubMed]

Watson, A. B. (1987). Estimation of local spatial scale. *Journal of the Optical Society of America A, Optics and Image Science, 4,* 1579–1582. [PubMed]

Whitaker, D., Latham, K., Mäkelä, P., & Rovamo, J. (1993). Detection and discrimination of curvature in foveal and peripheral vision. *Vision Research, 33,* 2215–2224. [PubMed]

Whitaker, D., Mäkelä, P., Rovamo, J., & Latham, K. (1992). The influence of eccentricity on position and movement acuities as revealed by spatial scaling. *Vision Research, 32,* 1913–1930. [PubMed]

Whitaker, D., Rovamo, J., MacVeigh, D., & Mäkelä, P. (1992). Spatial scaling of vernier acuity tasks. *Vision Research, 32,* 1481–1491. [PubMed]

Yager, D., & Davis, E. T. (1987). Variations of visual functions across the visual field: Introduction [Abstract]. *Journal of the Optical Society of America A, Optics and Image Science, 4,* 1478.